Alternating and Rotational Losses up to Magnetic Saturation in Non-Oriented Steel Sheets

Alternating and Rotational Losses up to Magnetic Saturation in Non-oriented Steel Sheets

Carlo Appino[1], Mahmood Khan[2], Olivier de la Barrière[3], Carlo Ragusa[2], and Fausto Fiorillo[1]

[1]Istituto Nazionale di Ricerca Metrologica (INRIM), Nanoscience and Materials Division, Strada delle Cacce 91, 10135 Torino, Italy
[2]Politecnico di Torino, Dipartimento Energia, Corso Duca degli Abruzzi 24, 10129 Torino, Italy
[3]SATIE, ENS Cachan, CNRS, UniverSud, 6, av. du President Wilson, F-94230 Cachan, France

A three-phase magnetizer has been developed, by which non-oriented Fe-Si steel sheets can be characterized under alternating and rotational flux up to polarisation value $J_p \approx 0.98\ J_s$, where J_s is the saturation magnetization. The measurements, performed in the frequency range 2 Hz 1 kHz, require combination of field-metric and thermo-metric methods, besides fine control of the induction wave-shape/loci under the required demanding exciting conditions. By exploiting the loss separation property it is observed that under rotational flux both the hysteresis and excess loss components eventually disappear at saturation and the measured losses become equal to the calculated classical losses. This could actually be predicted, because of the expected disappearance of the domain walls under saturating rotational field, but it has never been previously verified by the experiments.

***Index Terms*—Non-oriented materials, rotational losses, very high inductions, electrical machines.**

I. Introduction

The efficiency of the electrical machines has global impact, because they are responsible for about three quarters of the worldwide electrical energy consumption. Its improvement passes through good knowledge of the properties of the magnetic cores, namely the energy losses. Under standard operating conditions, the iron core is subjected to complex regimes, including two-dimensional (2D) fluxes, while being often driven to very high induction levels, close to magnetic saturation, typically in the teeth region of the stator core ([1] [2]). Because of obvious experimental difficulties, little results have been so far reported for such extreme working conditions, both under alternating and 2D flux [3] [4][5]. Consequently, machine designers are usually bound to extrapolate data obtained from measurements at medium induction levels, while having, at the same time, seldom access to 2D characterization. But knowledge of the material response as a function of the magnetizing frequency up to very high inductions has interest from a fundamental viewpoint, especially for rotational magnetization and its theoretical interpretation [6][7]. Quasi-static measurements on Fe-Si, typically performed with a torque balance, have actually shown that the parasitic torque (i.e. the energy loss) goes to zero on approaching the saturation, which is interpreted in terms of ensuing full disappearance of the domain walls [8][9]. We could expect that at power frequencies and beyond the measured loss at saturation would reduce to the classical loss component, but there are no experiments substantiating this assumption. Criticism regarding the conventional formulation of the classical losses has been raised in recent times [10]. CecchettiAt power We could reasonably expect that, It is stealso fundamental , besides these relevant Besides these important applicative There is further Furthermore, a wider experimental background would be of interest for the theoretical interpretation of rotational magnetization process This is a basic step in order to implement efficient numerical calculations needed for the design of electromagnetic devices.

To these end, two three-phase magnetizers were developed in order to explore the alternating and rotational loss behaviour in 0.35 mm thick non-oriented Fe-Si disk samples up to high induction ($B_p \simeq 2$ T) or in a wide frequency range, by combination of the thermo-metric and the field-metric methods, the last at lower B_p.In the rotational case, the condition at which the total loss reduces to the classical component has been obtained, so pointing out the complete disappearance of domain walls at high induction, as theoretically expected. In addition, it has been possible to perform the experimental analysis of the loss components, demonstrating the validity of the *Loss Separation* property even close to saturation. This approach, providing the values of the *Statistical Theory of Losses* (STL) parameters and the ratios between the rotational and alternating loss components, is basic to work out an exhaustive interpretation of the magnetisation process, whatever the flux loci, and to connect it to the material microstructure.

II. Experimental

Disk-shaped specimens (80 mm diameter), laser cut from a non-oriented Fe-(3.2wt%)Si lamination and annealed at 780°C for 2 hours in vacuum, have been characterised under alternating and rotational fluxes. The sample physical parameters are: electrical conductivity = 2.04 S/m, mass density = 7650 kg/m3, average grain size ⟨s⟩ = 92 m, specific heat per unit mass c_p = 462 J kg^{-1}K^{-1} (as obtained applying the Kopp-Neumann law), saturation polarisation $J_s = 2.01$ T, and thickness d = 0.356 mm. Two different digitally controlled Rotational Single Sheet Testers have been

Manuscript received April 1, 2015; revised May 15, 2015 and June 1, 2015; accepted July 1, 2015. Date of publication July 10, 2015; date of current version August 20, 2015. Corresponding author: C. Ragusa (e-mail: carlo.ragusa@polito.it). Color versions of one or more of the figures in this paper are available online at http://ieeexplore.ieee.org.
Digital Object Identifier (inserted by IEEE).

applied to measure hysteresis loops and losses under the desired flux locus. The first setup has been devised to reach frequencies up to about 5 kHz thanks to the optimisation of the magnetiser shape, obtained minimising the required apparent power at B_p = 1.5 T and 1 kHz, under rotating regime [7]. The field-metric method was applied in this case. The second excitation system has been designed by a similar procedure, but with the purpose to attain B_p = 1.95 T under rotating flux condition. As the thermometric technique is adopted in this last case, a vacuum chamber is housed between the specimen and the magnetiser. The maximal current (80 A) of the CROWN audio 5000VZ linear amplifiers is necessary to reach the required applied field. Measurements span the frequency f and peak induction B_p ranges 2Hz ≤ f ≤ 1kHz and 0.1T ≤ B_p ≤ 2T. The fieldmetric and thermometric methods are respectively exploited to cover the low (0.1T ≤ B_p ≤ 1.7T) and high (1.6T ≤ B_p ≤ 2 T) flux density range [4], [8]. The behaviour of loss vs. peak induction is displayed in Figs. 1 and 2 for the alternating ($W^{(ALT)}$) and the rotating ($W^{(ROT)}$) flux loci, respectively. An almost linear $W^{(ALT)}$ vs. B_p dependence is apparent at induction higher than 1.7 T, approximately, whereas one finds the typical maximum of $W^{(ROT)}$ around $B_p \simeq$ 1.5 T, followed by a pronounced drop, as saturation is approached.

III. Discussion

A. Behaviour of loss at high polarizations

In the following we will report the physical quantities as function of the relative peak polarisation J_p / J_s, that is the significant parameter when considering the magnetisation process. It is underlined that an appreciable difference can exist between $\boldsymbol{B}$ and $\boldsymbol{J} = \boldsymbol{B} - \mu_0 \boldsymbol{H}$ approaching saturation. The capability of the experimental setup to achieve polarization values very close to saturation, allowed us to display the behaviour of the rotational loss at high induction, an experimental condition scarcely investigated in the literature. Fig. 3 shows in particular the behaviour of the measured rotational loss $W^{(ROT)}$ vs. the relative peak polarisation at given values of the frequency. In the same Fig. 3 is also reported the computed classical loss component obtained under circular induction and peak induction B_p at frequency f:

$$W_{class}^{(ROT)} = 2 \cdot W_{class}^{(ALT)} = \pi^2 / 3\sigma d^2 B_p^2 f \qquad (\mathrm{J/m^3}). \tag{1}$$

Here, Eq. (1) is valid under uniform flux distribution, i.e. negligible skin effect. Following the procedure outlined in [10] it was possible to envisage the presence of the skin-effect beyond f = 300 Hz at high induction, a phenomenon that can be neglected in the present discussion, being the frequency limited to 200 Hz at such high inductions. It is remarkable the drop of $W^{(ROT)}$ (solid lines) up to the classical component at $J_p \simeq 1.96$ T $\simeq$ 0.98 J_s (corresponding to the induction upper limit $B_p \simeq 2$ T, shown in Figs. 1 and 2) because the disappearance of the domain walls under high fields.

This fact calls for the investigation of the behaviour of alternating and rotational loss vs. f and J_p, which can be discussed under the conceptual framework of the Loss Separation property, made general and applied to circular and alternating induction as well:

$$W = W_{hyst} + W_{class} + W_{exc}, \tag{2}$$

being W_{hyst} and W_{exc} the hysteresis and excess components [6]. To obtain the loss separation, component W_{hyst} could be retrieved, in principle, for a given flux loci (alternating or rotational) and peak induction, by extrapolation of Eq. (2) at f = 0. In addition, excess component could be obtained from (2) as $W_{exc} = W - W_{hyst} - W_{class}$. Nevertheless, the STL [6] applied to a generic elliptical flux locus provides the following expression for the excess component:

$$W_{exc} \cong g \cdot 8.76 \cdot \sqrt{\sigma G S V_0 J_p^3} \cdot \sqrt{f}, \tag{3}$$

where $G \simeq 0.1356$, S = 14.03 mm^2 is the measuring cross sectional area, V_0 a statistical parameter associated to the pinning field strength distribution, and g a factor depending on the flux locus shape (g = 1 and $g \approx 1.8$ for the alternating and the rotational case, respectively) [6]. In this way, from (2) we obtain:

$$W - W_{class} = W_{hyst} + g \cdot 8.76 \cdot \sqrt{\sigma G S V_o J_p^3} \cdot \sqrt{f}. \tag{4}$$

For a given value of the peak induction, Eq. (4) becomes a two-parameters expression, namely W_{hyst} and V_0, whose values can be obtained through the best fit of the experimental alternating and rotational loss vs. f curves.
In Fig. 4 is reported an example of the loss separation obtained at 50 Hz, under circular induction. It is remarkable the above mentioned reduction of $W^{(ROT)}$ (solid line) to the classical component (dashed line, Eq. (2)) at $J_p \simeq 1.96$ T $\simeq 0.98\ J_s$, and the corresponding vanishing of $W_{hyst}^{(ROT)}$ and $W_{exc}^{(ROT)}$.

B. Rotational vs. alternating loss

The phenomenological approach to the problem of loss under 2D fluxes is usually formulated in terms of the relationship existing between 2D and 1D behaviours, embodied in the ratios $R_{hyst}(J_p) = W_{hyst}^{(ROT)}/W_{hyst}^{(ALT)}$ and $R_{exc}(J_p) = W_{exc}^{(ROT)}/W_{exc}^{(ALT)}$, both depending on the peak induction. In addition. from Eq. (1) is found $R_{class} = W_{class}^{(ROT)}/W_{class}^{(ALT)} = 2$.

We therefore formulate the following phenomenological expression for the energy loss under rotating induction:

$$W^{ROT}(J_p, f) = R_{hyst}(J_p) \cdot W_{hyst}^{(ALT)}(J_p) + 2 \cdot W_{class}^{(ALT)}(J_p, f) + R_{exc}(J_p) \cdot W_{exc}^{(ALT)}(J_p, f). \tag{5}$$

Fig. 5a reports the evolution vs. J_p of the hysteresis energy

loss $W_{hyst}^{(ALT)}$ and $W_{hyst}^{(ROT)}$ obtained under alternating and rotating induction. In the same Fig. 5a is reported the ensuing ratio R_{hyst}.

The ratio of the excess loss component R_{exc} (J_p) is theoretically obtained from Eq. (3):

$$R_{exc}(J_p) \cong 1.8 \cdot \sqrt{V_0^{(ROT)} / V_0^{(ALT)}} \quad . \tag{6}$$

Fig. 5b reports the behaviour of the STL parameters $V_0^{(ALT)}$, $V_0^{(ROT)}$, and the theoretical ratio R_{exc} obtained through Eq. (6). In Fig. 6 we could eventually compare the theoretical excess ratio obtained from Eq. (6) to the corresponding measured ratio between the rotating and the alternating excess loss components vs. the reduced polarization, for different values of the frequency ranging from 20 Hz to 350 Hz. This comparison shows that the ratio R_{exc} is almost independent on frequency because the simultaneous dependence of $W_{exc}^{(ALT)}$ and $W_{exc}^{(ROT)}$ on the square root of frequency, in agreement with the theoretical prediction given by STL (Eq. (6)).

In principle, if some degree of uncertainty can be accepted, one could retrieve, for each J_p, the whole behaviour of W vs. f performing only two loss measurements at two frequencies, being only two parameters (W_{hyst} and V_0) needed (see Eq. (4)), so allowing loss prediction on a wide range of frequencies and inductions starting from minimal experimental set.

C. *Magnetization process and microstructure*

As a final point we want to envisage possible connections between magnetisation process and material microstructure, in the framework of STL, where only domain wall displacements are considered. In this model, magnetisation reversal is supposed to be driven by regions called *Magnetic Objects* (MOs), each accounting for the role played by a group of strongly interacting domain walls; in other words, one can think of a MO as a region with a rather homogeneous coercive field. As discussed in detail in [9], if assuming a box distribution of hysteresis fields H, of width $2\langle H_{hyst}\rangle$, one can work out an expression for the total number of MOs available for the reversal: $N_0 \simeq 2\langle H_{hyst}\rangle / V_0$. Taking, as a first guess, $\langle H_{hyst}\rangle \simeq W_{hyst}/(4J_p)$, and considering square MOs with average size $\square_{MO}$ one gets the formula

$$\lambda_{MO}(J_p) = \sqrt{S / N_0} \approx \sqrt{2SV_0 J_p / W_{hyst}(J_p)} \tag{7}$$

For $J_p < 0.75 \cdot J_s$, corresponding to the region before the maximum of the $W^{(ROT)}(B_p)$ curve (Fig. 2)) Eq. (8) provides $\square_{MO}^{(ALT)} \sim 90$ □m and $\square_{MO}^{(ROT)} \sim 65$ □m: values very close to the sample average grain size $\langle s \rangle = 92$ □m, obtained from micro-structural analysis. This fact suggest the possibility to identify MOs with the grains themselves, in agreement with the assumption that in fine-grained materials the main fluctuations of the coercive field are expected to take place from grain to grain.

IV. Conclusion

Thanks to expressly designed three-phase excitation systems, a complete magnetic characterisation of the loss behaviour in conventional non-oriented Fe-(3.2wt%)Si disk shaped steel laminations has been performed up to inductions very close to saturation, in a wide range of frequency both under alternating an rotational polarisation. This experimental background is basic for modelling and prediction of the material behaviour in condition often encountered in the rotating machine cores. The whole phenomenology has been interpreted in the framework of the Statistical Loss Theory. Particularly, it must be pointed out the ability of the equipment to reach, for the first time, the "*classical limit*", where the total rotational loss equals its classical component.

Acknowledgment

This work was supported in part by the MIUR Project TIVANO, grant CTN01 00236 256622, and by the French ANR project e-me□ca. The authors want to thank Michel Lècrivain and Patrice Vallade for valuable help in the development of the experimental setup.

References

[1] Y. Guo, J. G. Zhu, J. Zhong, H. Lu, J. X. Jin, "Measurement and Modeling of Rotational Core Losses of Soft Magnetic Materials Used in Electrical Machines: A Review", *IEEE Trans. Mag.*, vol. 44 (2), pp. 279□291, 2008.

[2] S. Steentjes, G. von Pfingsten, M. Hombitzer, K. Hameyer, "Iron-Loss Model With Consideration of Minor Loops Applied to FE-Simulations of Electrical Machines", *IEEE Trans. Mag.*, vol. 49 (7), pp. 3945□3948, 2013.

[3] T. Todaka, Y. Maeda, and M. Enokizono, "Counterclockwise/clockwise (CCW/CW) rotational losses under high magnetic field", *Prezglad Elektrotechniczny*, vol. 85, pp. 20-24, 2009.

[4] C. Appino, F. Fiorillo, C. Ragusa, B. Xie, "Magnetic losses at high flux densities in nonoriented Fe-Si alloys", *Journal of Magnetism and Magnetic Materials*, vol. 320, pp. 2526□2529, 2008.

[5] C. Appino, F. Fiorillo, and C. Ragusa, "One- dimensional/two-dimensional loss measurements up to high inductions", *Journal of Applied Physics*, vol. 105, pp. 07E718-1□07E718-3, 2009.

[6] M. J. Hofmann, H. Herzog, "Modeling Magnetic Power Losses in Electrical Steel Sheets in Respect of Arbitrary Alternating Induction Waveforms: Theoretical Considerations and Model Synthesis", *IEEE Trans. Mag.*, vol. 51 (2), pp. 6300211, 2015.

[7] C. Appino, C. Ragusa, and F. Fiorillo, "Can rotational magnetization be theoretically assessed?", *International Journal of Applied Electromagnetics and Mechanics*, vol. 44, pp. 355□370.

[8] F. Brailsford, "Alternating hysteresis loss in electrical sheet steels", *J. IEE,* vol. 84, pp. 399-407, 1939.

[9] K. Narita and T. Yamaguchi, "Rotational and alternating hysteresis losses in 4% silicon-ron single crystal with the {110} surface", *IEEE Trans. Mag.* vol. 11 (6), pp. 1661-1666, 1974.

[10] S.E. Zirka, Y.I. Moroz, P. Marketos, and A.J. Moses, "Loss separation in nonoriented electrical steels", *IEEE Trans. Mag.*, vol. 46 (2), pp. 286-289, 2010.

[11] A. Cecchetti, G. Ferrari, F. Masoli, and G.P. Soardo, "Rotational power losses in 3% SiFe as a function of frequency", *IEEE Trans. Mag.*, vol. 14 (5), pp. 356-358, 1978.

[12] O. de la Barrière, C. Appino, F. Fiorillo, F. Lècrivain, C. Ragusa, P. Vallade, "A novel magnetizer for 2D broadband characterization of steel sheets and soft magnetic composites", *International Journal of Applied Electromagnetics and Mechanics*, vol. 48, no. 2,3, pp. 239-245, 2015

[13] C. Ragusa, C. Appino, and F. Fiorillo, "Magnetic losses under two-dimensional flux loci in Fe□Si laminations", *Journal of Magnetism and Magnetic Materials*, vol. 316, pp. 454□457, 2007.

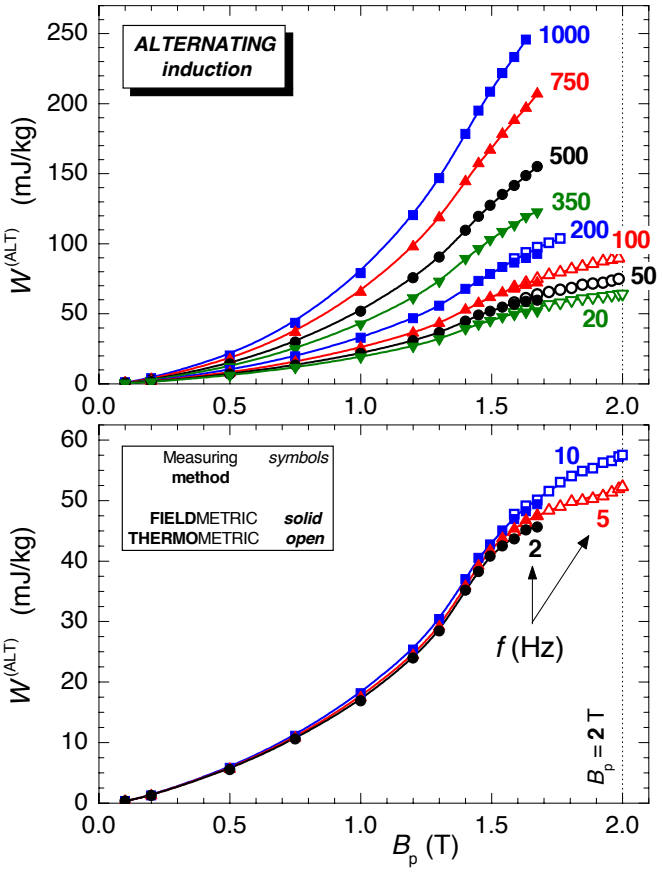

Fig. 1. Non-oriented Fe-(3.2wt%)Si disk sample: behavior, vs. peak induction, of the magnetic energy loss under alternating flux, with frequency spanning from 2 Hz to 1 kHz.

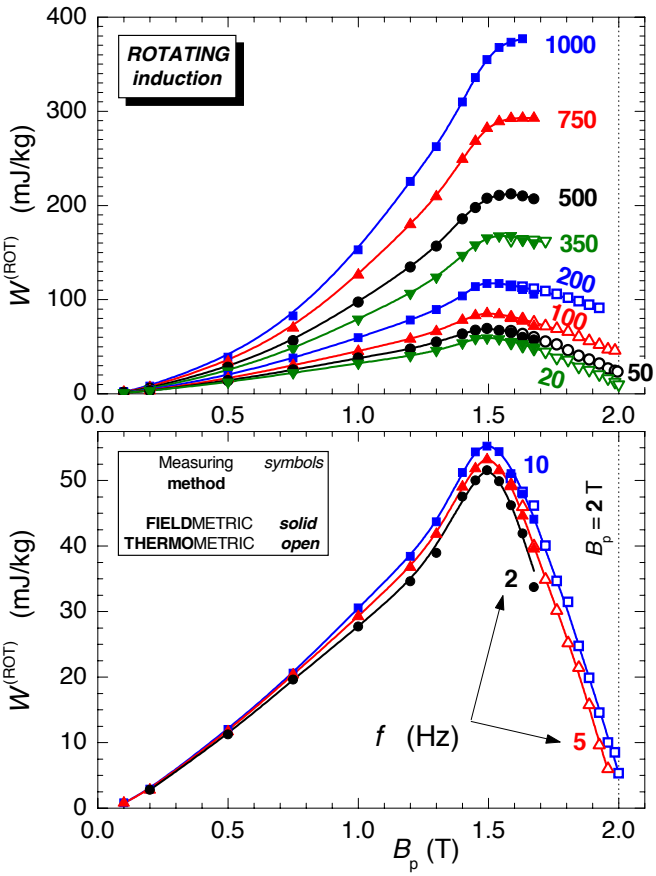

Fig. 2. Same as in Fig. 1, but under rotating flux.

[14] G. Bertotti, "Hysteresis in Magnetism", *Academic Press, New York*, (1998), Chap. 12.

[15] C. Appino, O. Hamrit, F. Fiorillo, C. Ragusa, O. de la Barrière, F. Mazaleyrat, M. LoBue, "Skin effect in steel sheets under rotating induction", *International Journal of Applied Electromagnetics and Mechanics*, vol. 48, no. 2,3, pp. 247-254, 2015.

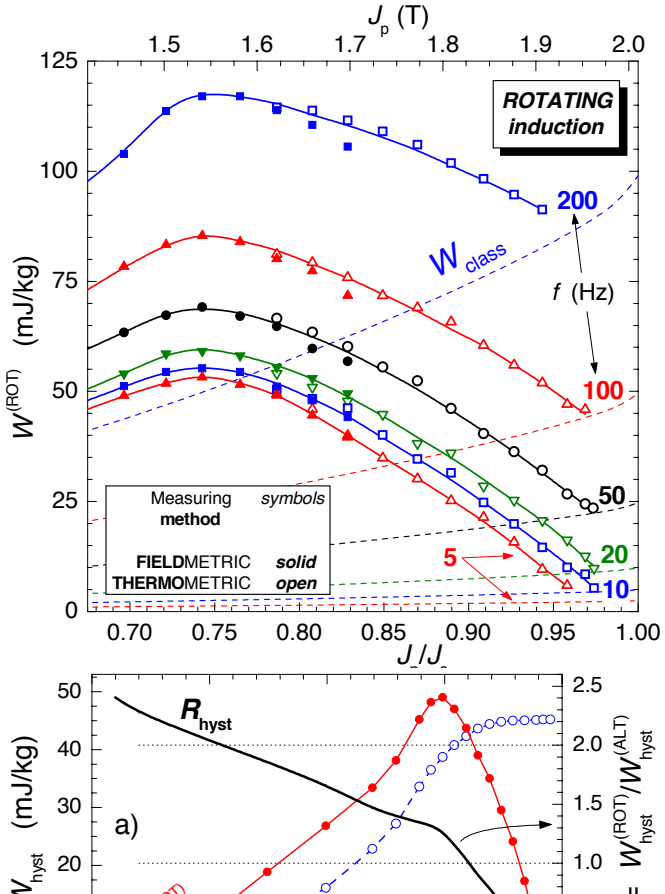

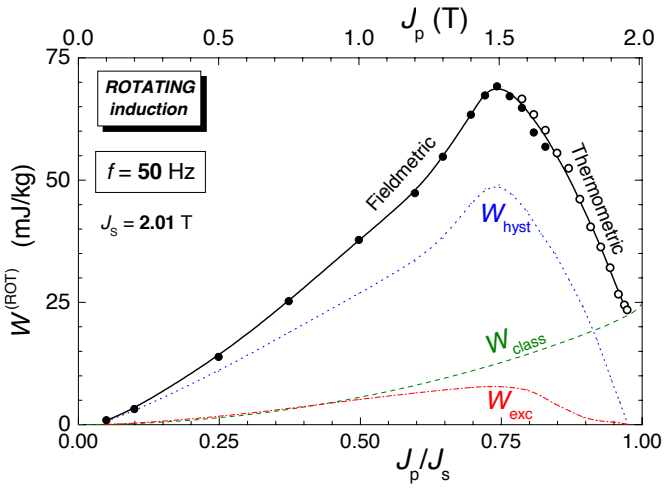

Fig. 4. Behaviour, at 50 Hz, of the rotational loss $W^{(ROT)}$ and its components. It is remarkable the drop of $W^{(ROT)}$(solid line) onto its classical component (dashed line, Eq. (2)) at $J_p \simeq 1.96$ T $\simeq 0.98\ J_s$, and the corresponding vanishing of $W_{hyst}^{(ROT)}$ and $W_{exc}^{(ROT)}$.

Figure aggiuntive

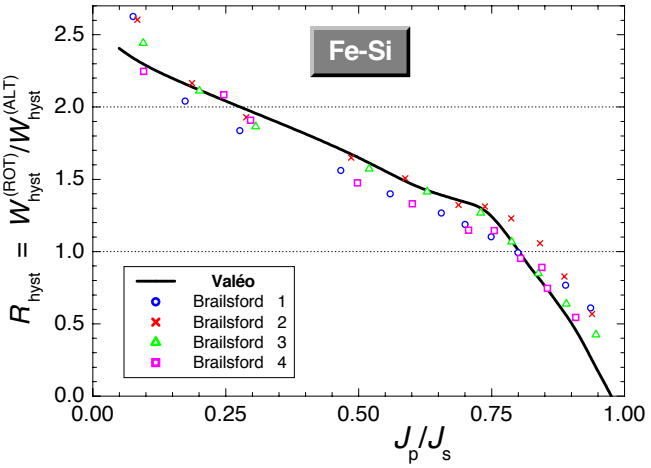

Fig. 7. Relation between rotational hysteresis loss and alternating hysteresis loss for the material under investigation (continuos line) compared to the same ratio obtained by Brailsford [xx] in four materials.

[xx] F. Brailsford, "Alternating hysteresis loss in electrical sheet steels", *J. IEE,* vol. 84, pp. 399-407, 1939.

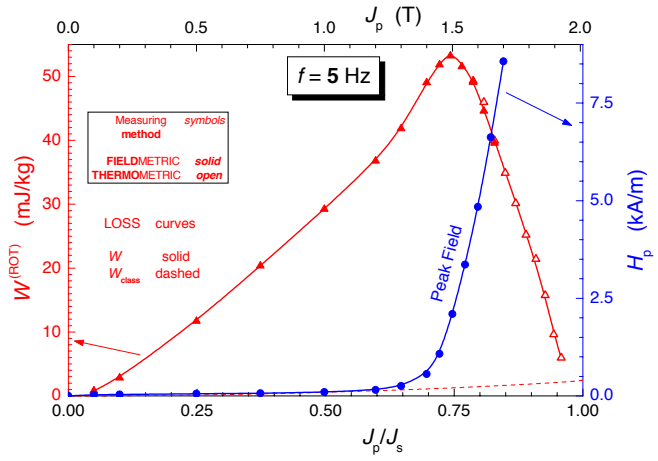

Fig. 8.